

RECENT ELECTRON-CLOUD SIMULATION RESULTS FOR THE MAIN DAMPING RINGS OF THE NLC AND TESLA LINEAR COLLIDERS*

M. Pivi[†], T. O. Raubenheimer, SLAC, Menlo Park 94025, California, USA
 M. A. Furman, LBNL, Berkeley 94720, California, USA

Abstract

In the beam pipe of the Main Damping Ring (MDR) of the Next Linear Collider (NLC), ionization of residual gasses and secondary emission give rise to an electron-cloud which stabilizes to equilibrium after few bunch trains. In this paper, we present recent computer simulation results for the main features of the electron cloud at the NLC and preliminary simulation results for the TESLA main damping rings, obtained with the code POSINST that has been developed at LBNL, and lately in collaboration with SLAC, over the past 7 years. Possible remedies to mitigate the effect are also discussed. We have recently included the possibility to simulate different magnetic field configurations in our code including solenoid, quadrupole, sextupole and wiggler.

INTRODUCTION

Beam induced multipacting, driven by the electric field of successive positively charged bunches, may arise from a resonant motion of electrons, generated by secondary emission, bouncing back and forth between opposite walls of the vacuum chamber. The electron-cloud effect (ECE) has been observed or is expected at many storage rings [1]. In all results presented, the positron beam is assumed to be a static distribution of given charge and shape moving at the center of the vacuum chamber, while the electrons are treated fully dynamically. We defer issues like the instability threshold, growth rate and frequency spectrum to future studies.

PHYSICAL MODEL

Sources of Electrons

In this article we consider what we believe to be the two main sources of electrons for the positron damping rings: (1) residual gas ionization and (2) secondary emission from electrons hitting the walls.

Secondary Emission Process

The secondary electron yield (SEY) $\delta(E_0)$ and the corresponding emitted-electron energy spectrum $d\delta/dE$ (E_0 = incident electron energy, E = emitted secondary energy) are represented by a detailed model described elsewhere [2]. The parameters have been obtained from detailed fits to the measured SEY of various materials [3]. Due to electron

Table 1: Simulation parameters for the NLC and TESLA positron damping rings.

Parameter	Symbol	NLC	TESLA
Beam energy	E , GeV	1.98	5.0
Bunch population	$N_p \times 10^{10}$	0.75	2
Ring circumference	C , m	299.8	17000
Dipole field	B , T	0.67	-
Quadrupole gradient	G , T/m	35	-
Wiggler field at max.	B_y , T	2.1	-
Wiggler period	λ_w , m	0.27	-
Bunches per train	N_b	192	2820
Train gap	τ_g , ns	65	-
Bunch spacing	b_s , ns	1.4	20
Bunch length ($\pm 5\sigma_z$)	σ_z , mm	5.5	6.0
Gauss. tr. bunch size	σ_x, σ_y μm	49, 6	230, 230
Beam pipe semi-axes	a, b cm	2, 2	5, 5
Antechamber gap	h , mm	10	none
No. slices/bunch	N_k	250	300
Steps during bunches	N_g	1400	200

scrubbing, the secondary electron yield is expected to decrease according to [4]. The main SEY parameters are the energy E_{max} at which $\delta(E_0)$ is maximum, the peak value $\delta_{\text{max}} = \delta(E_{\text{max}})$ and the elastic backscattered and rediffused components of the secondary emitted-electron energy spectrum $d\delta/dE$ at $E_0 \simeq 0$.

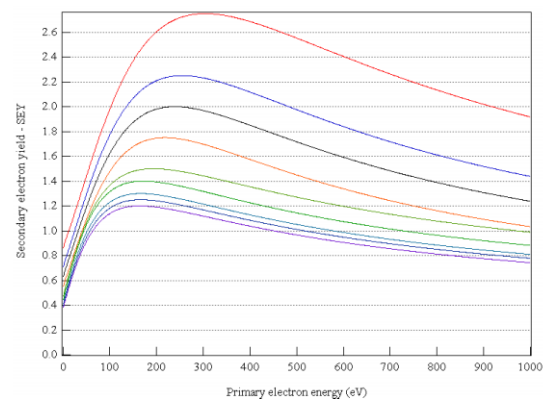


Figure 1: Secondary electron yield model used for the simulations.

Simulation Model

The NLC positron MDR stores 3 trains, separated by 65 nsec with each train consisting of 192 bunches having a 1.4

* Work supported by the US DOE under contracts DE-AC03-76SF00515 and DE-AC03-76SF00098.

[†] mpivi@slac.stanford.edu

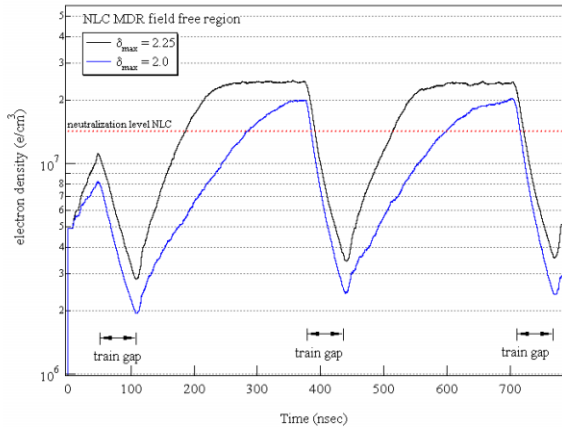


Figure 2: Development of the electron cloud during the passage of two bunch trains in a NLC Main Damping Ring field free region. Simulations for secondary yield δ_{max} 2.25 and 2.0, with an initial seed of the electrons $5 \times 10^6 e/cm^3$. The dependence of the saturation level with the SEY is shown in Fig 3.

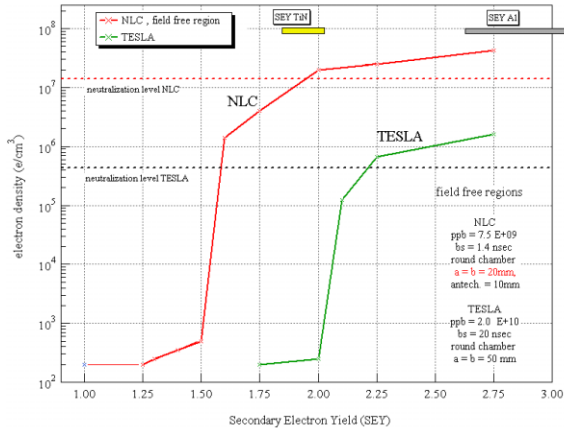


Figure 3: Dependence of the saturation density level with the peak SEY in a field free region of the NLC and TESLA Main Damping Ring. Typical value ranges for the SEY of Aluminum and TiN coated *as received* samples are shown above in the figure.

nsec bunch spacing. The aluminum vacuum chamber is assumed to be a cylindrical perfectly-conducting round pipe with a 20 mm radius and includes an antechamber to remove most of the synchrotron radiation. The TESLA main damping ring stores 2820 bunches with a 20 nsec bunch spacing. The vacuum chamber in the long TESLA straight sections is a round aluminum pipe with a 50 mm radius without an antechamber.

Typically, the electrons are simulated by macro-particles, each one representing a defined number of electrons and carrying a fixed charge. The secondary electron emission mechanism adds to these a variable number of macro-particles, generated according to the SEY model mentioned above. The bunch is divided up into N_k slices

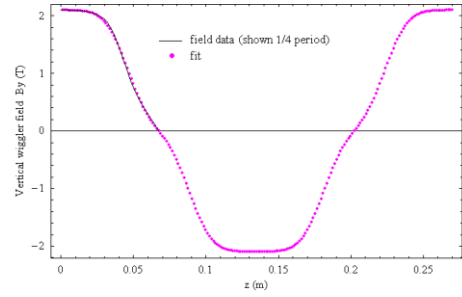


Figure 4: Wiggler vertical field model, NLC MDR.

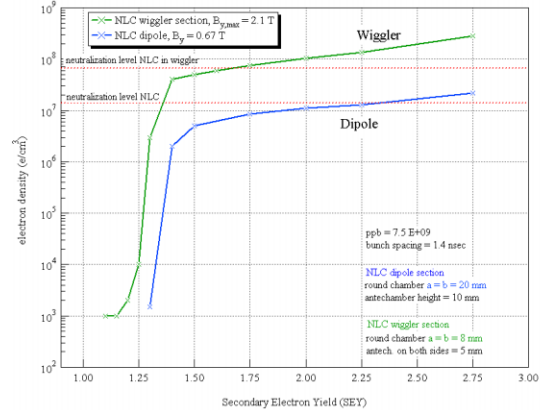


Figure 5: Saturation density as a function of δ_{max} in a NLC wiggler (above) and a dipole section. Thresholds for the development of the electron cloud are respectively $\delta_{max} \sim 1.3$ and 1.4. Note that the neutralization level in a wiggler is higher due to a smaller beam pipe cross section.

and the inter-bunch gap into N_g intermediate steps. The image and space charge forces are computed and applied at each slice in the bunch and each step in the gap. Typical beam and vacuum chamber parameters are listed in Table 1.

Since each bunch generates a small number of electrons by ionization of residual gases, a simulation of the entire process, up to the saturation level, would require a large number of macro-particles and long computer processing time. The saturation density level depends on the electron cloud space charge forces, the secondary electron yield and is independent of the initial seed. Thus, we generate a large number of electrons at the first bunch passage and let the electron cloud develops until a saturation density is reached, see Fig. 2.

SIMULATION RESULTS

NLC and TESLA Ring Field Free Regions

In our study, we are mainly interested in the estimate of the saturation electron density as a function of the secondary yield. The simulation results for the field free regions in both damping rings are shown in Fig. 3. The threshold for the development of the electron cloud in a field free region is $\delta_{max} \sim 1.6$ and 2.1 for NLC and TESLA,

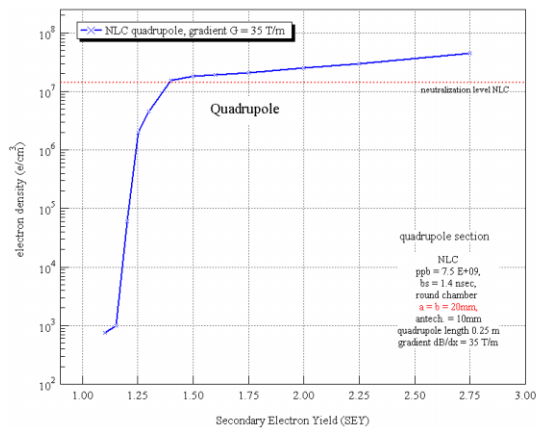


Figure 6: Saturation density as a function of the peak secondary yield in an NLC MDR quadrupole.

respectively. The threshold should occur under the conditions where the production rate of secondary electrons exceeds the decay rate of the electron cloud. The neutralization levels are also shown in figure.

NLC Dipole, Quadrupole and Wiggler

We have recently included in our code the possibility to simulate different magnetic field configurations. We present simulation results for the electron cloud in the wiggler, quadrupole and dipole regions of the NLC positron main damping ring.

For analysis of the electron dynamics in a wiggler, we have used a cylindrical mode representation of the field [5] and a model for the wiggler field used in our simulation is shown in Fig. 4. In the wiggler, an 8mm radius round beam pipe is provided with antechamber on both sides $h_w=5$ mm. We simulate a four period section of the wiggler. The results are compared with the results for a dipole region in Fig. 5.

The saturation density as a function of the secondary yield in a quadrupole are shown in Fig. 6. We generate the electrons in a 0.25 m long quadrupole with field gradient $G=35$ T/m. Previous studies and simulations [6] indicate that electrons may be trapped in a quadrupole, therefore surviving a long gap between bunch trains. The electron cloud decay times for three different sections are shown in Fig. 7. Note that, in these simulations, our code does not consider longitudinal variation of the quadrupole field which is treated as infinitely long¹. Refined quadrupole simulations are underway.

CONCLUSIONS

We present electron cloud simulation results suggesting that the SEY threshold for the development of the electron cloud in the main damping rings field free regions is

¹This is a good approximation, if the effective net flow of electrons leaving the quadrupole region is small.

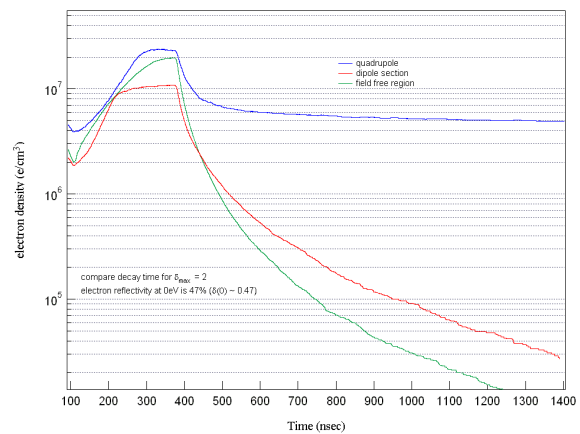


Figure 7: Decay time of the electron cloud compared for three different sections of the NLC MDR. Trapping of the electrons in the quadrupole field may result in a long decay time. Note that, in these simulations, our code does not consider the longitudinal variation of the quadrupole field, the quadrupole should be considered infinitely long.

$\delta_{\max} \sim 1.6$ and 2.1 respectively for the NLC and TESLA. Furthermore, we simulate the electron cloud effect in the dipole, wiggler and quadrupole of the NLC main damping ring. A demanding SEY threshold is given by $\delta_{\max} \sim 1.3$ in the wigglers. Simulations confirm the electron trapping mechanism in quadrupoles. More simulations are needed to estimate the longitudinal drift of the electrons in quadrupoles.

We are considering TiN as a possible coating material to reduce the secondary yield of aluminum. An experimental program, to measure the secondary yield of TiN coating materials and study the reduction of the SEY due to ion sputtering of the TiN surface, has started at SLAC. Furthermore, the solenoid field is a possible way to suppress the electron cloud in a limited fraction of the damping rings.

We are particularly grateful to our colleagues for many stimulating discussions, especially to A. Wolski, F. Le Pimpec and R. Kirby. We are grateful to NERSC for supercomputer support.

REFERENCES

- [1] For an updated summary and links on electron cloud studies, see ELOUD02: <http://slap.cern.ch/collective/ecloud02/>. In particular, see contributions from: N. Hilleret, R. Macek, K. Harkay, M. Blaskiewicz, K. Ohmi, F. Zimmermann.
- [2] M.A. Furman, M. Pivi Phys.Rev. ST AB **5**, 124404, 2002.
- [3] R. Kirby, private communication.
- [4] J.M. Jimenez et al. LHC-Project-Report-632.
- [5] M. Venturini, A. Wolski, A. Dragt these proceedings RPAB023.
- [6] L. Wang presentation <http://conference.kek.jp/two-stream/>; F. Zimmermann, CERN SL-Note-2002-017 (AP); P. J. Channell and A. J. Jason, LANL AOT-3 Tech. Note 94-11.